J Biol Inorg Chem
DOI 10.1007/s00775-016-1339-x

ORIGINAL PAPER

Zinc oxide and titanium dioxide nanoparticles induce oxidative stress, inhibit growth, and attenuate biofilm formation activity of *Streptococcus mitis*

Shams Tabrez Khan[1,2] · Javed Ahmad[1,2] · Maqusood Ahamed[3] · Javed Musarrat[4] · Abdulaziz A. Al-Khedhairy[2]

Received: 24 November 2015 / Accepted: 7 January 2016

Abstract *Streptococcus mitis* from the oral cavity causes endocarditis and other systemic infections. Rising resistance against traditional antibiotics amongst oral bacteria further aggravates the problem. Therefore, antimicrobial and antibiofilm activities of zinc oxide and titanium dioxide nanoparticles (NPs) synthesized and characterized during this study against *S. mitis* ATCC 6249 and Ora-20 were evaluated in search of alternative antimicrobial agents. ZnO and TiO_2-NPs exhibited an average size of 35 and 13 nm, respectively. The IC_{50} values of ZnO and TiO_2-NPs against *S. mitis* ATCC 6249 were 37 and 77 μg ml^{-1}, respectively, while the IC_{50} values against *S. mitis* Ora-20 isolate were 31 and 53 μg ml^{-1}, respectively. Live and dead staining, biofilm formation on the surface of polystyrene plates, and extracellular polysaccharide production show the same pattern. Exposure to these nanoparticles also shows an increase (26–83 %) in super oxide dismutase (SOD) activity. Three genes, namely *bap*A1, *sod*A, and *gtf*B like genes from these bacteria were identified and sequenced for quantitative real-time PCR analysis. An increase in *sod*A gene (1.4- to 2.4-folds) levels and a decrease in *gtf*B gene (0.5- to 0.9-folds) levels in both bacteria following exposure to ZnO and TiO_2-NPs were observed. Results presented in this study verify that ZnO-NPs and TiO_2-NPs can control the growth and biofilm formation activities of these strains at very low concentration and hence can be used as alternative antimicrobial agents for oral hygiene.

Keywords ZnO · TiO_2 · Nanoparticles · Oral hygiene · Alternative antimicrobials · *S. mitis*

Introduction

Oral bacteria pose a serious health challenge as an etiological agent of several systemic infections besides dental and periodontal diseases [1]. Emerging antibiotic resistance among these bacteria further aggravates the problem of oral hygiene and of systemic diseases resulting from recurring oral infections [2]. Infections of *Streptococcus mitis*, a commensal oral bacterium, and a low virulence pathogen lead to endocarditis, sepsis in neutropenic patients, toxic shock like syndrome, and pancreatic cancer [3–6]. Moreover, the incidence of multidrug resistance in *S. mitis* including resistance to β-lactams, tetracycline, and aminoglycosides is a matter of concern [7, 8]. Whole genome sequence and other studies also confirm the presence of genetic information for multidrug resistance in *S. mitis* [9]. Therefore, it is of immense importance to minimize the population of *S. mitis* in the oral cavity and/or to control other systemic infections caused by this bacterium using alternative antimicrobial agents.

Electronic supplementary material The online version of this article (doi:10.1007/s00775-016-1339-x) contains supplementary material, which is available to authorized users.

✉ Shams Tabrez Khan
shamsalig75@gmail.com

1 DNA Research Chair, Zoology Department, College of Science, King Saud University, Riyadh 11451, Saudi Arabia

2 Zoology Department, College of Science, King Saud University, P.O. Box 2455, Riyadh 11451, Saudi Arabia

3 King Abdullah Institute for Nanotechnology, King Saud University, Riyadh 11451, Saudi Arabia

4 Department of Agricultural Microbiology, Faculty of Agricultural Sciences, Aligarh Muslim University, Aligarh 202002, India

Published online: 02 February 2016

Nanoparticles exhibit excellent antimicrobial activities [10–13] and are being already used in a number of commercial products including toothpaste, sunscreen, and food products [14, 15]. One such nanoparticle with a global production of 5500 tons per year and with excellent antimicrobial activity is TiO_2-NPs [15, 16]. TiO_2-NPs are used in various food products with EU code E171, and the average exposure for an adult in the USA is estimated to be 1 mg Ti per kilogram body weight per day [17]. Another important metal oxide nanoparticle with excellent antimicrobial activity is ZnO [11, 12]. In addition to possessing antimicrobial activity, nanoparticles are inexpensive and biocompatible and hence can be used as novel front-line alternative/complementary antimicrobial agents [18, 19]. However, only a few studies have checked the antimicrobial activity of these nanoparticles on viridian group of streptococci with relevance to oral health. Furthermore, the mechanism underlying their antimicrobial activity is not well understood. This study, therefore, aims to describe the antimicrobial and antibiofilm activity of ZnO- and TiO_2- NPs against *S. mitis* and elaborates the possible mechanism of their antimicrobial activity.

Materials and methods

Synthesis and characterization of TiO_2- and ZnO-nanoparticles

Anatase TiO_2 nanoparticles were synthesized by the simple hydrothermal method of Castro et al. [20]. Briefly, 10 % solution (w/w) of titanium trichloride ($TiCl_3$) prepared in 20 % w/w HCl was diluted 1:2 in 2 M HCl. To this diluted solution, 4 M ammonium was added dropwise until a white precipitate appeared. This suspension was maintained at room temperature overnight and was washed with deionized water to remove excess ammonium and chloride ions. Crystallization of TiO_2 precursor was carried out with pure water in an autoclave at 200 °C for 2 h. ZnO-NPs were synthesized from zinc acetate dihydrate (Merck chemicals) by the sol–gel method [21].

X-ray diffraction (XRD) patterns were determined to check the crystalline nature of the synthesized nanoparticles. The XRD pattern were acquired at room temperature with the help of a PANalytical X'Pert X-ray diffractometer (Spectris plc, England) equipped with a Ni filter using Cu Kα ($\lambda = 1.54056$ Å) radiations as an X-ray source. Size and structures of nanoparticles were determined by field emission transmission electron microscopy (FETEM, JEM-2100F, JEOL Inc., Japan) at an accelerating voltage of 200 kV. For FETEM analysis, homogeneous suspensions of nanoparticles in water (100 µg/ml) were prepared by sonication at room temperature for 15 min at 40 W. The particle size distribution of nanoparticles was determined by dynamic light scattering (DLS) using ZetaSizer-HT (Malvern, UK).

Bacterial strains and culture media

Two strains of *Streptococcus mitis* were used in this study. *Streptococcus mitis* ATCC 6249 was obtained from the American type culture collection. Another isolate of *Streptococcus mitis*, Ora-20 was isolated from the oral cavity of a healthy male (age 40 years) and was characterized using polyphasic approaches including 16S rRNA gene sequencing and biochemical tests. For routine culture, brain heart infusion broth (BHI; Mast Group, Bootle, UK) with 2 % sucrose was used. Strains were stored at −80 °C in 20 % glycerol for longer preservation and storage.

Polyphasic characterization of the strains

Polyphasic characterization of Ora-20 was carried out as described by Khan et al. [22]. Briefly, for determining 16S rRNA gene sequences, lysate from exponentially growing cells was prepared using Prepman ultra (Applied Biosystems) according to the protocol of supplier. 16S rRNA gene was amplified with a pair of universal primers, 27f, and 1492r, as described by Khan et al. [22]. Amplicons were sequenced using an ABI PRISM 3100 Genetic Analyzer 3130 (Applied Biosystems, Foster City, CA, USA) and BigDye Terminator v3.1 Cycle Sequencing Kit, according to the manufacturer's instructions. Partial sequences determined using 27F and 536R primers were assembled and compared with those available in NCBI, DNA databank using the basic local alignment search tool (BLAST). Production of H_2O_2, and acid from lactose, melibiose, and raffinose, and hydrolysis of urea were checked using the standard protocols described by Cowan and Steel [23].

Antimicrobial activity of ZnO and TiO_2 nanoparticles

Cultures of both *Streptococcus mitis* isolates (ATCC 6249 and Ora-20) were grown overnight in BHI broth with 2 % sucrose. Aliquots of 500 µl were added to 5 ml of sterile BHI broth containing different concentrations (25, 50, 100 and 200 µg ml^{-1}) of ZnO-NPs or TiO_2. Broths without any nanoparticle were used as a control. The cultures were incubated at 37 °C for 12 h and appropriate dilutions of treated and untreated cells were spread on BHI agar plates. The plates were incubated at 37 °C for 3 days, and the numbers of colony-forming units (CFUs) were determined and presented as $\log_{10}$ CFU/ml.

Live and dead staining

Both ATCC 6249 and Ora-20 were grown with 50 µg ml^{-1} of ZnO-NPs and 100 µg ml^{-1} of TiO_2-NPs to exponential phase (8 h) in individual experiments. Exponentially growing cultures of the treated and untreated isolates were harvested by centrifugation at 915×*g* and suspended in autoclaved PBS buffer (pH 7.5). Populations of live and dead cells in these samples were determined using the LIVE/DEAD® BacLight™ Bacterial Viability Kit (Molecular probes-Life technologies, USA), following manufacturer's instructions. Stained cells were observed under a fluorescence microscope (Nikon Eclipse 80i; Nikon Co., Japan). Twelve fields for each treatment were counted and the percentage of dead cells was calculated by comparing the number of cells stained with propidium iodide to those stained with SYTO 9 in the same field.

Quantitative assessment of biofilm formation

Quantitative inhibition of biofilm formation in the presence of TiO_2 and ZnO -NPs was assessed on 48-well polystyrene plates (Nunc, Denmark) as described by Burton et al. [24]. Sterile BHI broths containing four concentrations (25, 50, 100 and 200 µg/ml) of TiO_2 and ZnO-NPs each were inoculated with the log phase cultures of ATCC 6249 and Ora-20. Cultures without any nanoparticles were taken as control. Plates were incubated at 37 °C for 16 h. The medium containing suspended cells was gently and completely removed and wells were washed three times with 500 ml of PBS buffer (137 mM NaCl, 2.7 mM KCl, 10 mM $Na_2HPO_4{\cdot}2H_2O$, 2 mM KH_2PO_4, pH 7.4). Plates were stained with 500 µl of 0.4 % crystal violet (CV) dye for 15 min at room temperature. The unbound dye was subsequently removed by gently washing the wells three times with 500 µl of PBS buffer. The CV retained by the biofilm was solubilized in 500 µl of 33 % acetic acid. Absorption was read at 620 nm using a microtitre plate reader (Multiskan Ascent, Labsystems, Helsinki, Finland).

Extracellular polysaccharide (EPS) production assay

The method described by Packiavathy et al. [25] was used to study the inhibition of EPS production. Freshly grown bacterial culture was added to 5 ml of sterile BHI broth amended individually with TiO_2 or ZnO-NPs at increasing concentrations of 25, 50, 100 and 200 µg/ml. EPS produced by NP-treated and untreated bacteria was measured as follows. Cultures were centrifuged at 12,298×*g* for 15 min and resuspended in autoclaved PBS (pH 7.0). The cell suspension was centrifuged again for 30 min at 13,559×*g* and EPS in the supernatant was precipitated with 3 volumes of 95 % ethanol and the precipitate was suspended in 500 µl of sterile Milli-Q water. For EPS quantification to 1 volume of EPS solution, 1 volume of ice-cold 5 % phenol and 5 volumes of concentrated sulphuric acid were added to develop a red color. The intensity of the color was measured spectrophotometrically at 490 nm.

Superoxide dismutase (SOD) assay

Cell suspensions prepared above were incubated with ZnO (30 µg ml^{-1}) and TiO_2-NPs (100 µg ml^{-1}) for 4 h at 37 °C. Following treatment, the cell suspensions were centrifuged for 12,298×*g* for 15 min. Cells were lysed with trichloroacetic acid (TCA, Sigma-Aldrich). Nitro blue tetrazolium (NBT, Invitrogen) was added to a final concentration of 0.45 mM and samples were incubated at 37 °C for an additional 30 min. Finally, the absorbance of the samples was recorded at 450 nm using a microplate reader (Multiskan Ascent, Labsystems, Helsinki, Finland) to measure the NBT diformazan formed in the samples.

Quantitative real-time PCR of the genes involved in biofilm and oxidative stress

For the quantitative real-time PCR studies four primer sets detailed in supplementary Table 1 were used. Total RNA from bacterial cells treated with ZnO (30 µg ml^{-1}) and TiO_2-NPs (100 µg ml^{-1}) for 12 h was extracted using RNeasy mini Kit (Qiagen) according to the manufacturer's instructions. Cells without any NPs were taken as control. The concentration of the extracted RNA was determined using Nanodrop 8000 spectrophotometer (Thermo-Scientific) and the integrity of RNA was visualized on 1 % agarose gel using gel documentation system (Universal Hood II, BioRad). The first-strand cDNA was synthesized from 1 µg of total RNA by Reverse Transcriptase using M-MLV (Promega) and random hexamer primer according to the manufacturer's protocol. Real-time quantitative PCR (RT-PCRq) was performed using LightCycler® 480 (Roche Diagnostics, Rotkreuz, Switzerland) and the SYBR Green I Master mix recommended by Roche (Cat # 04707516001, Roche Diagnostics, Switzerland). Two microliters of template cDNA was added to the final volume of 20 µl of the reaction mixture. Real-time PCR cycle parameters included

Table 1 Sizes of synthesized TiO_2 and ZnO nanoparticles estimated using TEM, XRD, and DLS analysis

Nanoparticle	Size (nm)		Hydrodynamic size (nm)		
	TEM	XRD	NPs concentration (µg ml^{-1})		
			50	100	200
ZnO	35	35	176	191	292
TiO_2	13.4	13	1272	1314	1802

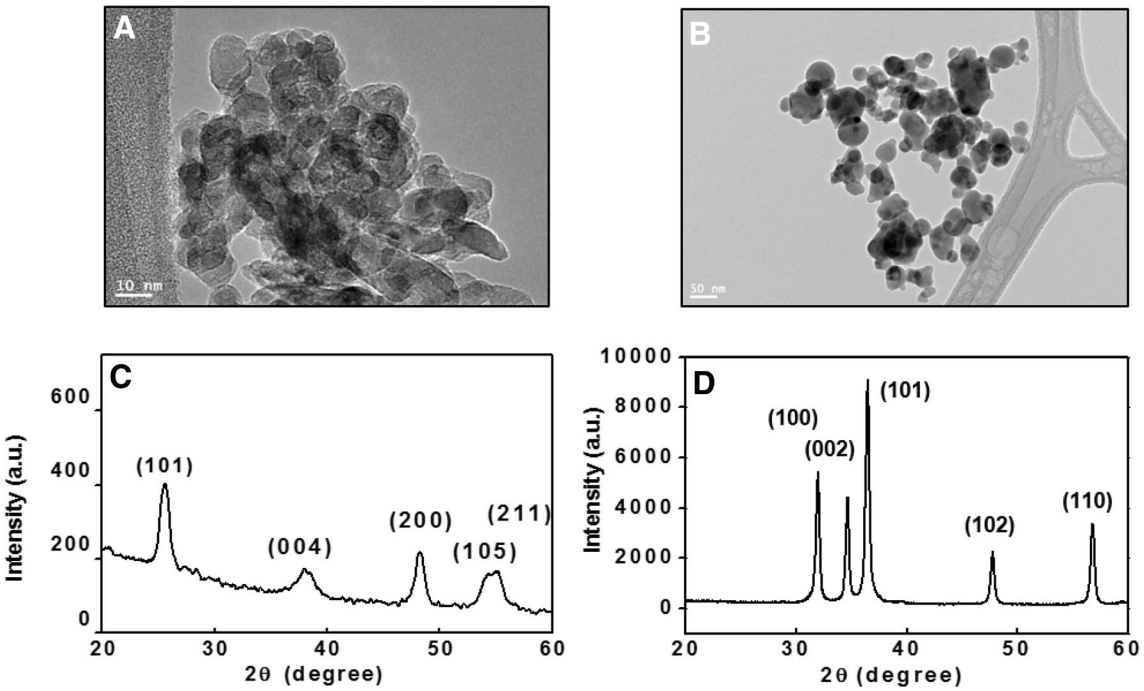

Fig. 1 Transmission electron microscopy (TEM) and X-ray diffraction patterns of TiO_2-NPs and ZnO-NPs. TEM images show anatase TiO_2-NPs (**a**), polygonal ZnO-NPs (**b**) and their respective XRD patterns in figure **c** and **d**

10 min at 95 °C followed by 40 cycles involving denaturation at 95 °C for 15 s, annealing at 60 °C for 20 s and elongation at 72 °C for 20 s. All the real-time PCR experiments were performed in triplicate and data expressed as the mean of at least three independent experiments.

Results and discussion

Synthesis and characterization of ZnO- and TiO_2-nanoparticles

Figure 1a shows the typical TEM image of TiO_2-NPs. The average size of TiO_2-NPs was calculated from measuring over 75 nanoparticles in random fields of view. The mean ± SD of TiO_2 nanoparticles was 13.43 ± 4.18 nm. The XRD pattern of the as-synthesized TiO_2-NPs sample is shown in Fig. 1c. Sharp diffraction peaks of the nanopowder corresponding to (101), (004), (200), (105) and (211) crystal planes were observed. These diffraction peaks are well defined and can be perfectly assigned to the anatase TiO_2 (JCPDS-21-1272). The absence of any impurity peaks suggested the high quality of anatase TiO_2 nanoparticles. The crystallite size of 13 nm has been estimated from the XRD pattern using the Scherrer's equation [26], supporting the TEM data (Table 1).

TEM image of ZnO-NPs synthesized by the sol–gel method [21] is shown in Fig. 1b. The ZnO-NPs were polygonal in shape with smooth surfaces and an average size of 35 ± 2.98 nm. The X-ray diffraction peaks of ZnO-NPs at (100), (002), (101), (102) and (110) suggest a polycrystalline wurtzite structure (Zincite, JCPDS5-0664). Although the size of TiO_2-NPs was smaller than that of ZnO-NPs, TiO_2-NPs exhibit largest hydrodynamic particle size (1272–1802 nm) in ultra-pure water in DLS analysis, than that of ZnO-NPs (176–292 nm; Table 1).

Polyphasic characterization of isolate Ora-20

The partial sequence of 16S rRNA gene of isolate Ora-20 submitted in DNA data bank of Japan (DDBJ; accession no. LC068581) shares 99 % similarity with the 16S rRNA gene of *Streptococcus mitis* ATCC 15914. Both the isolate Ora-20 and strain ATCC 6249 produce H_2O_2, and produce acid from lactose, melibiose and raffinose, but did not hydrolyze urea. These biochemical tests show that the isolate Ora-20 actually belongs to the species *Streptococcus mitis*, confirming the results of 16S rRNA gene sequence analysis [27].

ZnO- and TiO_2-NPs mediated change in growth and viability of *S. mitis*

The antimicrobial activity of ZnO- and TiO_2-NPs against *S. mitis* isolate Ora-20 and ATCC 6249 is shown in Fig. 2. It is clear from the figure that ZnO-NPs exhibit higher

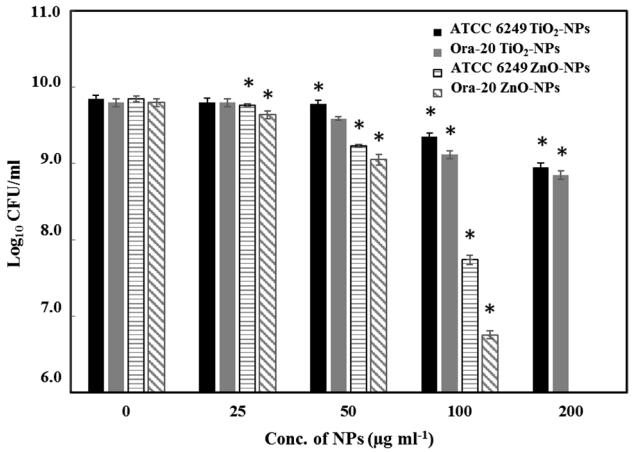

Fig. 2 Antimicrobial activity of TiO_2-NPs and ZnO-NPs against ATCC 6249 and Ora-20. It is to be noted that ZnO-NPs exhibit significant growth inhibition (*p value <0.005) of both organisms even at 25 μg ml^{-1}. The values presented are mean ± SD of two independent experiments done in triplicate

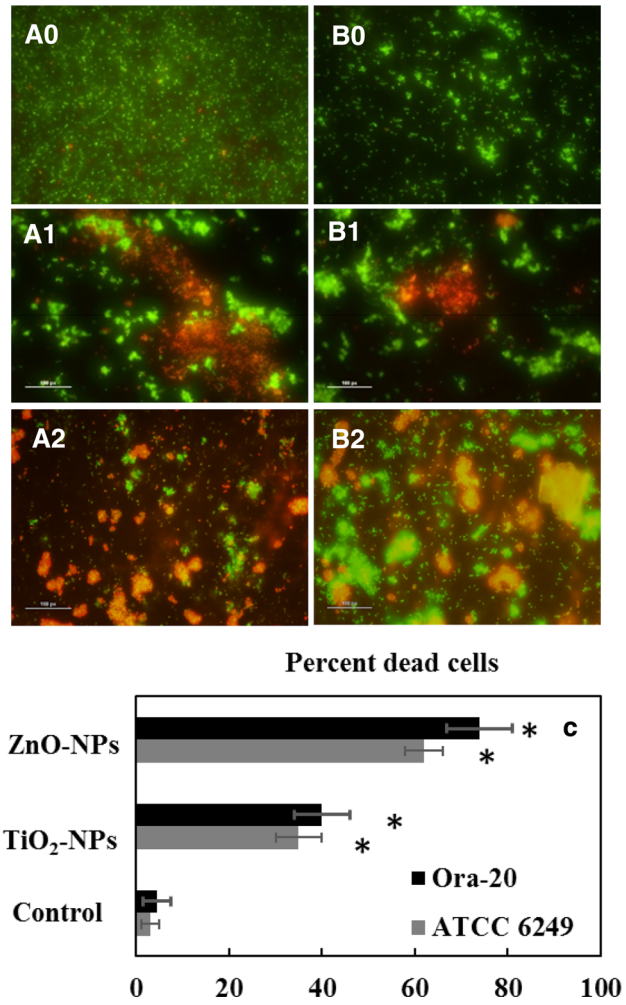

Fig. 3 Population of live (*green*) and dead (*orange*) cells estimated using BacLight Kit following treatment with ZnO (50 μg ml^{-1}) and TiO_2-NPs (100 μg ml^{-1}). Figs. **a0** and **b0**, show the populations of live and dead cells of ATCC 6249 and Ora-20 in control cultures. Population of dead cells of ATCC 6249 increased significantly following treatment with TiO_2-NPs and ZnO-NPs as shown in fig **a1** and **a2**, respectively. Figure **b1** and **b2** shows the increase in the population of dead cells of Ora-20 following treatment with TiO_2-NPs and ZnO nanoparticles, respectively, while *panel* **c** shows the *bar graph* of percent dead cells (mean ± SD of 12 fields) after treatment with nanoparticles (*p value <0.005)

antimicrobial activity than TiO_2-NPs, against both the test organisms. A decrease of 99 % in the colony-forming units of both organisms was observed when grown with 100 μg ml^{-1} of ZnO-NPs, while a decrease of only 68 and 79 % in the populations of ATCC 6249 and Ora-20, respectively, was observed with the same concentration of TiO_2-NPs (100 μg ml^{-1}). ZnO-NPs exhibited an IC_{50} value of 37.05 and 31.7 μg ml^{-1} against ATCC 6249 and Ora-20, respectively, while TiO_2-NPs exhibited much higher IC_{50} values of 77 and 53.29 μg ml^{-1} against ATCC 6249 and Ora-20, respectively, further confirming that isolate Ora-20 is more sensitive to these nanoparticles than the strain ATCC 6249.

The results of viability assay also show that ZnO-NPs more effectively decrease the viability of the test bacteria than TiO_2-NPs (Fig. 3). Images 4A0 and 4B0, show the live/dead staining of ATCC 6249 and Ora-20, respectively, grown without any nanoparticles. The number of dead cells of ATCC 6249 and Ora-20 increased from 3 ± 2 (A0) and 4.5 ± 3 % (B0) in controls to 35 ± 5 % (A1) and 40 ± 6 % (B1), respectively, when grown with 100 μg ml^{-1} of TiO_2-NPs, while the population of dead cells of ATCC 6249 and Ora-20 increased to 62 ± 4 and 74 ± 7 %, respectively, with 50 μg ml^{-1} of ZnO-NPs. Increased staining with propidium iodide following treatment with nanoparticles indicate disruption of cell walls of the bacterium resulting in death.

Although, antimicrobial activities of ZnO-NPs against a number of oral bacteria has been reported [28, 29], to the best of our knowledge the antimicrobial activity of metal and metal oxide NPs except for silver NPs against *S. mitis* has not been determined [30]. The antimicrobial activity of silver NPs [30] was found to be size dependent, wherein the smallest NPs (5 nm) exhibited highest antimicrobial activity with an MIC value of 25 μg ml^{-1}. In our study presented above, both ZnO- and TiO_2-NPs show significant antimicrobial activity even at low concentrations against ATCC 6249 and Ora-20. Although the size of ZnO-NPs (35 nm) was three times that of TiO_2-NPs (13 nm), ZnO-NPs exhibit superior antimicrobial activity than TiO_2-NPs. The higher antimicrobial activity of ZnO-NPs compared to TiO_2-NPs has been reported earlier also [28]. Furthermore, hydrodynamic size of TiO_2-NPs (1272–1802 nm) in our

study was four to six times bigger than that of ZnO-NPs (176–292 nm). The antimicrobial activity of NPs may also be due to the release of metal ions from these nanostructures. Dimpka et al. [31] have shown the release of Zn ions (2.8–7.5 %) from ZnO-NPs which was found to increase with a decrease in the pH. It is to be noted that both bacteria produce acid and result in a decrease of pH during the growth (data not shown). The release of Ti metal from TiO_2-NPs has also been demonstrated, but the percentage of Ti metal released from NPs was comparatively lower (0.53–0.82 %) than that of ZnO [32]. The poor antimicrobial activity of TiO_2-NPs may be due to this low concentration of Ti metal released from TiO_2-NPs and a bigger hydrodynamic size.

ZnO-NPs and TiO_2-NPs mediated biofilm inhibition of *S. mitis*

The biofilm formation activity of *S. mitis* ATCC 6249 and Ora-20 on the surface of polystyrene plates was inhibited by both the nanoparticles, i.e. ZnO- and TiO_2-NPs in a concentration-dependent manner (Fig. 4). An inhibition of 4.2 ± 3, 11.8 ± 4, 18.6 ± 5 and 27.6 ± 6 % of the biofilm formation by ATCC 6249 was observed with 25, 50, 100 and 200 μg ml^{-1} of TiO_2-NPs, respectively, while the corresponding values for ZnO-NPs were 7, 20, 40 and 46.7 %. The biofilm formation activity of isolate Ora-20 was reduced by 11.5 ± 4, 23.3 ± 4, 30.2 ± 6 and 37.3 ± 8 % when grown with 25, 50, 100 and 200 μg ml^{-1} of TiO_2-NPs, respectively. while ZnO-NPs reduced the biofilm formation activity of Ora-20 by 12.8 ± 4, 25.2 ± 5, 65.9 ± 8 and 74.8 ± 9 % at a concentration of 25, 50, 100 and 200 μg ml^{-1}, respectively. Significant inhibition (p value <0.05) of biofilm formation activity of ATCC 6249 and Ora-20 was observed at 50 μg ml^{-1} of ZnO-NPs, while, TiO_2-NPs inhibited the biofilm formation by ATCC 6249 and Ora-20, significant (p value <0.05) at a concentration of 100 and 50 μg ml^{-1}, respectively, which again confirms that ZnO-NPs are more effective than TiO_2-NPs at inhibiting the biofilm formation activity of *S. mitis*.

Biofilm formation by oral bacteria is crucial to oral hygiene. ZnO-NPs have been shown to inhibit biofilm formation activity of various oral bacteria including *Streptococcus sobrinus* ATCC 27352, *Rothia* sp. and *Streptococcus mutans* and total oral bacteria [12, 13, 33, 34]. NPs may percolate through the spaces between bacteria disrupting biofilm mechanically and killing bacteria by inhibiting biochemical processes crucial to biofilm formation such as exopolysaccharide production [13]. ZnO-NPs exhibit better antibiofilm activity than TiO_2-NPs, again probably due to the higher quantity of Zn ions than Ti metal ions produced by their respective nanoparticles [31, 32]. It has been demonstrated that charge of the nanoparticles plays an important role in their diffusion through a biofilm [35]. Metal ions from NPs also inhibit enzymes, such as *Dap*E, involved in the later stages of peptidoglycan synthesis adversely affecting biofilm formation [36]. Very few studies on the TiO_2-NPs mediated inhibition of oral biofilm are available [37].

TiO_2- and ZnO-NPs induced inhibition of EPS production

Both the NPs, namely TiO_2- and ZnO-NPs reduced the production of EPS by *S. mitis* ATCC 6249 and Ora-20 (Fig. 5). It is evident from the figure that a significant (p value <0.05) inhibition of EPS production by Ora-20 was observed only with 20 μg ml^{-1} of ZnO and TiO_2-NPs,

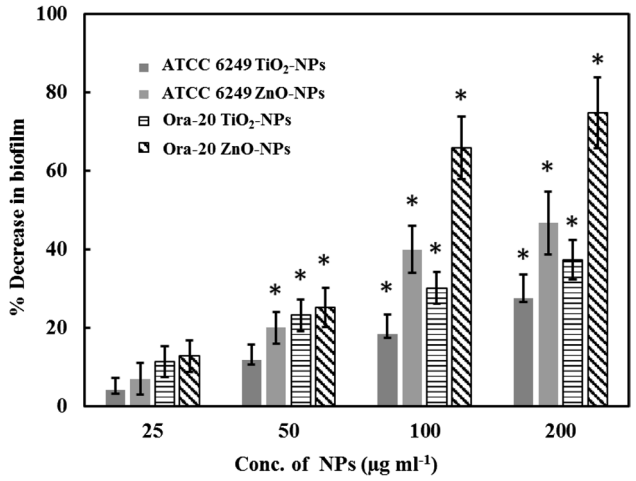

Fig. 4 Percent decrease in the biofilm formation activities of ATCC 6249 and Ora-20 in the presence of TiO_2-NPs and ZnO-NPs on the surface of polystyrene plates as compared to control. *Represents the p value <0.05

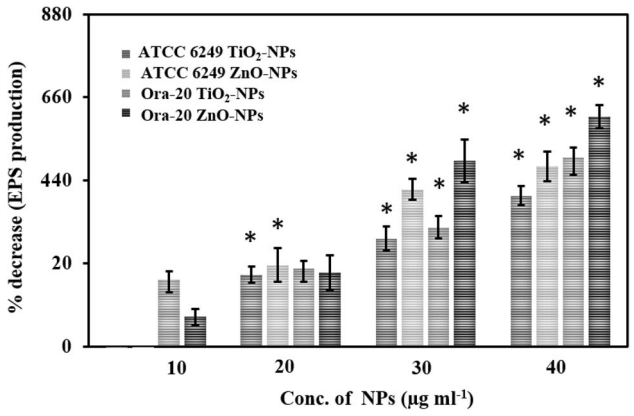

Fig. 5 TiO_2 and ZnO-NPs mediated concentration-dependent change in the EPS production by *S. mitis* (ATCC 6249 and Ora-20). *Represents the p value <0.05

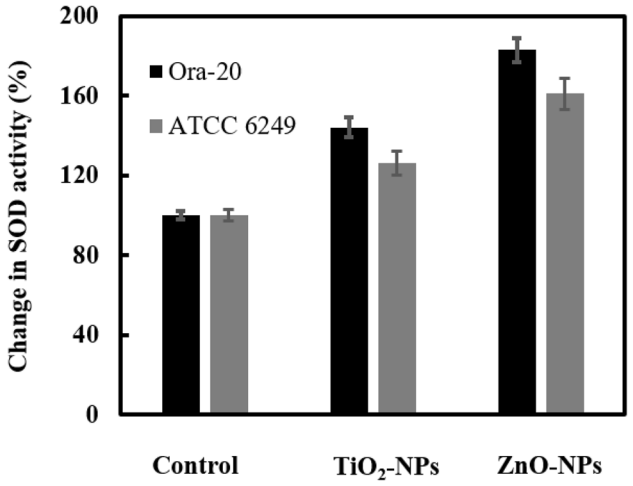

Fig. 6 Increase in the SOD activities of ATCC 6249 and Ora-20 when grown with TiO_2-NPs and ZnO-NPs. *Represents the *p* value <0.05

while this significant inhibition (*p* value <0.05) of EPS production by ATCC 6249 was observed only with 30 µg ml^{-1} or higher concentration of tested NPs, therefore showing that Ora-20 was more sensitive to the tested nanoparticles than ATCC 6249. NPs mediated inhibition of EPS production by bacteria has been documented earlier also [12]. Inhibition of enzymes involved in the production of EPS such as glucosyltransferase by metal ions has been demonstrated in vitro [38].

Superoxide dismutase (SOD) assay

The change in SOD activity, when grown with NPs, is shown in Fig. 6. Compared to control, an increase of 26 and 61 % in the SOD activity of ATCC 6249 when grown with of TiO_2- and ZnO-NPs, respectively, was observed. The corresponding increase in the SOD activity of Ora-20 upon growth with the TiO_2- and ZnO-NPs was 44 and 83 %, respectively. These results clearly show that ZnO-NPs and TiO_2-NPs both induce oxidative stress in ATCC 6249 and Ora-20. Nanoparticle-mediated induction of oxidative stress in bacteria has been demonstrated earlier also [39]. ZnO- and TiO_2-NPs induced oxidative stress in *E. coli* was reported by Kumar et al. [40]. Amongst oral bacteria, ZnO-NPs cause oxidative stress and increased the activity of SOD in *Streptococcus mutans* [34].

Molecular study and gene expression

Gene amplification and validation

A total of three primer sets targeting (supplementary Table 1) superoxide dismutase (*sod*A) gene, biofilm-associated protein-like gene (*bap*A1 like) and glycosyltransferase B (*gtf*B) gene were used for gene expression studies. These genes were selected to study the change in oxidative stress level (*sod*A), biofilm formation activity (*bap*A1 like), and the change in the production of EPS (*gtf*B). Partial sequences of *sod*A genes from viridian group of *Streptococci* are already available in DNA data bank (NCBI), and a primer set for the gene has also been published earlier [41]. *sod*A genes, therefore, were amplified using the primer set and PCR conditions described by Johnston et al. [41]. For sequencing also, the PCR primers were used unless mentioned otherwise. The sequences of *sod*A genes from ATCC 6249 and Ora-20 were submitted to DNA databank of Japan (DDBJ) with accession numbers LC068582 and LC068584, respectively. The *sod*A gene sequence obtained from ATCC 6249 shows 96 % sequence similarity to the *sod*A gene of *Streptococcus* sp. IE45 (Accession no. KF288804), while the sequences obtained from Ora-20 share a sequence similarity of 99 % with *Streptococcus* sp. IE44 (Accession no. KF288803). A PCR fragment of *gtf*B gene c.a. 286 bp was amplified using the primer set described in supplementary Table 1. Sequences of this amplicon from ATCC 6249 and Ora-20 were also submitted to DDBJ with accession numbers LC068583 and LC068585, respectively. The sequence of the *gtf*B gene from ATCC 6249 shares a similarity of 93 % with the *gtf*B gene of *Streptococcus salivarius* (FR873481), while the sequence from Ora-20 shares a similarity of 90 % with the *gtf*B gene of *Streptococcus salivarius* (FR873481). Genes similar to biofilm-associated protein were also identified in *S. mitis*, as the *bap*A1 like gene in *S. mitis* (EJG87516) shares 67 % similarity with *Streptococcus parasanguinis* (JF345716). Based on the primary analysis amplicon of c.a. 173 bp wa obtained from ATCC 6249 and Ora-20 as expected (data not shown). But we failed to obtain the sequences of these amplicons.

Gene expression studies by RT-PCR

The change in gene expression levels (*sod*A and *gtf*B) following treatment with nanoparticles is shown in Fig. 7. Data were normalized by 16S rRNA gene. The expression level of *sod*A gene increased by 2.5- and 1.6-folds when the cells of Ora-20 and ATCC 6249 were grown with 30 µg ml^{-1} of ZnO-NPs, respectively. The corresponding increase in *sod*A gene expression of Ora-20 and ATCC 6249, when grown with 100 µg ml^{-1} TiO_2-NPs, was 2.14- and 1.43-folds. The increase in *sod*A gene levels, when grown with nanoparticles, confirms the results of SOD assays, wherein the growth of tested isolates with nanoparticles results in 26–83 % increase in SOD activity. The expression levels of *gtf*B gene decreased by 0.93- and 0.89-folds in ATCC 6249 and Ora-20 upon growth with

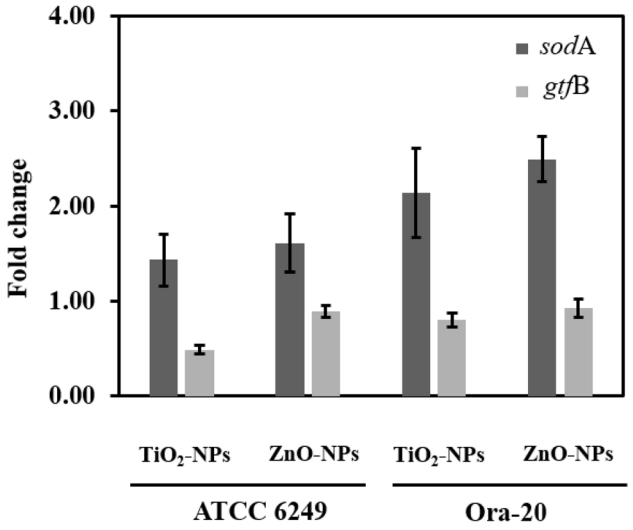

Fig. 7 Change in gene expression levels of *sod*A and *gtf*B genes in ATCC 6249 and Ora-20 when grown with TiO_2-NPs and ZnO-NPs

30 μg ml^{-1} of ZnO-NPs. When grown with 100 μg ml^{-1} of TiO_2-NPs the expression levels of *gtf*B gene decreased by 0.49- and 0.8-folds in ATCC 6249 and Ora-20, respectively (Fig. 7). A significant decrease in the EPS production by ATCC 6249 and Ora-20 was also observed even with 20 μg ml^{-1} of tested nanoparticles. The significant decrease in biofilm formation activity of ATCC 6249 and Ora-20 with ZnO-NPs and TiO_2-NPs supports the results of gene expression studies. Although a decrease in *bap*A1 gene expression levels was also observed, but as the sequence reaction for this gene failed, finding on this gene will remain inconclusive.

ZnO-NP mediated cell wall disruption and oxidative stress were found to be the main mode of action against *Campylobacter jejuni* [42]. Reverse transcription-quantitative PCR analysis of *Campylobacter jejuni* showed that in response to ZnO-NPs' (~35) treatment the expression levels of two oxidative stress genes (*kat*A and *ahp*C) and a general stress response gene (*dna*K) increased by 52-, 7-, and 17-fold, respectively [42]. Our studies presented above also show increased permeability of propidium iodide, increased SOD activity and increased expression of *sod*A gene following the treatment with nanoparticles. These results suggest that treatment with tested NPs results in oxidative stress and disruption of the cell wall in ATCC 6249 and Ora-20. Hence, the synthesized nanoparticles can be used to control the growth and biofilm formation activity of oral bacteria.

As the use of these NPs for controlling oral *Streptococci* is proposed, it is important to carefully and realistically evaluate the nanotoxicity of ZnO and TiO_2-NPs. Although these NPs may not exert acute adverse effects to human cells, due to the short exposure time and non-toxic doses, in vitro cytotoxicity of ZnO-NPs against a number of cell lines is reported [43]. On the contrary, very few reports on the in vivo toxicity of these nanoparticles are available and this remains a subject of future studies. It has been demonstrated that ZnO-NPs (8-10 nm) and TiO_2-NPs (5 nm) both show minimal toxicity below 100 μg/cm^2 [44]. Vandebriel and De-Jong in their review on mammalian toxicity of ZnO-NPs have concluded that in vitro toxicity of ZnO-NPs is largely due to the oxidative stress [45]. They have also concluded that the genotoxicity of ZnO-NPs was only observed in in vitro studies and not in in vivo studies. As our results suggest the use these NPs at much lower concentration (~50–70 μg ml^{-1}), toxicity arising from any accidental ingestion will be insignificant.

Conclusions

Results presented in this study clearly demonstrate that TiO_2- and ZnO-NPs exhibit marked antimicrobial and antibiofilm activity against ATCC 6249 and Ora-20 and hence can control their growth and biofilm formation activity in the oral cavity even at a concentration as low as 50 μg ml^{-1}. Results presented above suggest that the antimicrobial and antibiofilm formation activity is due to the disruption of the cell wall and oxidative stress. Therefore, these nanoparticles can be used as alternative antimicrobial agents against oral opportunistic pathogen *Streptococcus mitis*.

Acknowledgments This work was supported by Al-Jeraisy Chair for DNA Research, King Saud University, Riyadh, Saudi Arabia.

Conflict of interest Authors have no conflict of interest whatsoever.

References

1. Han YW, Wang X (2007) J Dent Res 92:485–491
2. Sweeney LC, Dave J, Chambers PA, Heritage J (2004) J Antimicrob Chemother 53:567–576
3. Rapeport KB, Girón JA, Rosner F (1986) Arch Intern Med 146:2361–2363
4. Balkundi DR, Murray DL, Patterson MJ, Gera R, Scott-Emuakpor A, Kulkarni R (1997) J Pediatr Hematol Oncol 19:82–85
5. Lu HZ, Weng XH, Zhu B et al (2003) J Clin Microbiol 41:3051–3055
6. Farrell JJ, Zhang L, Zhou H et al (2012) Gut 61:582–588
7. König A, Reinert RR, Hakenbeck R (1998) Microb Drug Resist 4:45–49
8. Doern GV, Ferraro MJ, Brueggemann AB, Ruoff KL (1996) Antimicrob Agents Chemother 40:891–894
9. Poutanen SM, de Azavedo J, Willey BM, Low DE, MacDonald KS (1999) Antimicrob Agents Chemother 43:1505–1507
10. Allaker RP (2010) J Dent Res 89:1175–1186
11. Khan ST, Ahmad M, Al-Khedhairy AA, Musarrat J (2013) Mater Lett 97:67–70
12. Khan ST, Ahamed M, Musarrat J, Al-Khedhairy AA (2014) Eur J Oral Sci 122:397–403

13. Khan ST, Al-Khedhairy AA, Musarrat J (2015) J Nanopart Res 17:276
14. Berube DM, Searson EM, Morton TS, Cummings CL (2010) Nanotechnol Law Bus 7:152–163
15. Piccinno F, Gottschalk F, Seeger S (2012) J Nanopart Res 14:1109–1120
16. Kubacka A, Diez MS, Rojo D et al (2014) Sci Rep 4:4134
17. Weir A, Westerhoff P, Fabricius L, von Goetz N (2012) Environ Sci Technol 46:2242–2250
18. Li Q, Mahendra S, Lyon DY et al (2008) Water Res 42:4591–4602
19. Seyedmahmoudi SH, Harper SL, Weismiller MC, Haapala KR (2015) J Nanopart Res 17:104
20. Castro AL, Nunes MR, Carvalho AP, Costa FM, Florêncio MH (2008) Solid State Sci 10:602–606
21. Raja M, Shanmugaraj AM, Ryu SH (2008) J Nanosci Nanotechnol 8:4224–4226
22. Khan ST, Harayama S, Tamura T et al (2009) Int J Syst Evol Microbiol 59:2094–2098
23. Cowan ST, Steel KJ (1993) Manual for the identification of medical bacteria, 3rd edn. Cambridge University Press, London
24. Burton E, Yakandawala N, LoVetri K, Madhyastha MS (2007) J Ind Microbiol Biotechnol 34:1–4
25. Packiavathy IASV, Priya S, Pandian SK, Ravi AV (2012) Food Chem 002. http://dx.doi.org/10.1016/j.foodchem.08
26. Patterson AL (1939) Phys Rev 56:978–982
27. Beighton D, Hardie JM, Whiley RA (1991) J Med Microbiol 35:367–372
28. Vargas-Reus MA, Memarzadeh K, Huang J, Ren GG, Allaker RP (2012) Int J Antimicrob Agents 40:135–139
29. Hernández-Sierra JF, Ruiz F, Pena DC et al (2008) Nanomedicine 4:237–240
30. Lu Z, Rong K, Li J, Yang H, Chen R (2013) J Mater Sci Mater Med 24:1465–1471
31. Dimpka CO, Calder A, Britt DW, McLean JE, Anderson AJ (2011) Environ Pollut 159:1749–1756
32. Soto-Alvaredo J, Blanco E, Bettmer J et al (2014) Metallomics 6:1702–1708
33. Aydin-Sevinc AB, Hanley L (2010) J Biomed Mater Res B 94:22–31
34. Eshed M, Lellouche J, Matalon S et al (2012) Langmuir 28:12288–12295
35. Peulen TO, Wilkinson KJ (2011) Environ Sci Technol 45:3367–3373
36. Uda NR, Upert G, Angelici G, Nicolet S, Schmidt T, Schwede T (2013) Metallomics 6:88–95
37. Chun MJ, Shim E, Kho EH et al (2007) Angle Orthod 77:483–488
38. Wunder D, Bowen WH (1999) Arch Oral Biol 44:203–214
39. Hwang ET, Lee JH, Chae YJ et al (2008) Small 2008(4):746–750
40. Kumar A, Pandey AK, Singh SS, Shanker R, Dhawan A (2011) Free Radic Biol Med 51:1872–1881
41. Johnston C, Hinds J, Smith A, Van-der-Linden M, van Eldere J, Mitchell TJ (2010) J Clin Microbiol 48:2762–2769
42. Xie Y, He Y, Irwin LP, Jin T, Shi X (2011) Appl Environ Microbiol 77:2325–2331
43. De Berardis B, Civitelli G, Condello M et al (2010) Toxicol Appl Pharmacol 246:116–127
44. Moos PJ, Olszewski K, Honeggar M et al (2011) Metallomics 3:1199–1211
45. Vandebriel RJ, De Jong WH (2012) Nanotechnol Sci Appl 5:61–71